tvst

DOI: 10.1167/tvst.6.6.1

Article

A Temporal White Noise Analysis for Extracting the Impulse Response Function of the Human Electroretinogram

Andrew J. Zele[1], Beatrix Feigl[2,3], Pradeep K. Kambhampati[2], Avinash Aher[4], Declan McKeefry[5], Neil Parry[5,6], John Maguire[5], Ian Murray[6], and Jan Kremers[4,5,7]

[1] Visual Science Laboratory, Institute of Health and Biomedical Innovation, School of Optometry and Vision Science, Queensland University of Technology (QUT), Brisbane, Australia
[2] Medical Retina Laboratory, Institute of Health and Biomedical Innovation, School of Biomedical Sciences, Queensland University of Technology (QUT), Brisbane, Australia
[3] Queensland Eye Institute, South Brisbane, Australia
[4] Laboratory for Retinal Physiology, Department of Ophthalmology, University Hospital Erlangen, Erlangen, Germany
[5] University of Bradford, Bradford School of Optometry and Vision Sciences, West Yorkshire, UK
[6] Vision Science Centre, Manchester Royal Eye Hospital, Central Manchester University Hospitals NHS Foundation Trust, Manchester Academic Health Science Centre, Manchester, UK
[7] Department of Anatomy II, Friedrich-Alexander University Erlangen Nürnberg, Erlangen, Germany

Correspondence: Andrew J. Zele, Institute of Health and Biomedical Innovation, QUT, 60 Musk Avenue, Kelvin Grove, Queensland 4059, Australia. e-mail: andrew.zele@qut.edu.au; Beatrix Feigl, Institute of Health and Biomedical Innovation, QUT, 60 Musk Avenue, Kelvin Grove, Queensland 4059, Australia. e-mail: b.feigl@qut.edu.au; Jan Kremers, University Hospital Erlangen, Schwabachanlage 6, 91054 Erlangen, Germany. email: jan.kremers@uk-erlangen.de

Received: 7 August 2017
Accepted: 23 September 2017
Published: 1 November 2017

Keywords: electroretinogram (ERG); temporal white noise; impulse response function

Citation: Zele AJ, Feigl B, Kambhampati PK, Aher A, McKeefry D, Parry N, Maguire J, Murray I, Kremers J. A temporal white noise analysis for extracting the impulse response function of the human electroretinogram. Trans Vis Sci Tech. 2017; 6(6):1, doi:10.1167/tvst.6.6.1

Purpose: We introduce a method for determining the impulse response function (IRF) of the ERG derived from responses to temporal white noise (TWN) stimuli.

Methods: This white noise ERG (wnERG) was recorded in participants with normal trichromatic vision to full-field (Ganzfeld) and 39.3° diameter focal stimuli at mesopic and photopic mean luminances and at different TWN contrasts. The IRF was obtained by cross-correlating the TWN stimulus with the wnERG.

Results: We show that wnERG recordings are highly repeatable, with good signal-to-noise ratio, and do not lead to blink artifacts. The wnERG resembles a flash ERG waveform with an initial negativity (N1) followed by a positivity (P1), with amplitudes that are linearly related to stimulus contrast. These N1 and N1-P1 components showed commonalties in implicit times with the a- and b-waves of flash ERGs. There was a clear transition from rod- to cone-driven wnERGs at ~1 photopic cd.m^{-2}. We infer that oscillatory potentials found with the flash ERG, but not the wnERG, may reflect retinal nonlinearities due to the compression of energy into a short time period during a stimulus flash.

Conclusion: The wnERG provides a new approach to study the physiology of the retina using a stimulation method with adaptation and contrast conditions similar to natural scenes to allow for independent variation of stimulus strength and mean luminance, which is not possible with the conventional flash ERG.

Translational Relevance: The white noise ERG methodology will be of benefit for clinical studies and animal models in the evaluation of hypotheses related to cellular redundancy to understand the effects of disease on specific visual pathways.

Introduction

Until now, the ERG has been measured mainly to flashed stimuli as an approximation of a delta function with a theoretically infinitesimal short time and infinite high energy over time of unity. It therefore approximates the impulse response function (IRF).[1,2] The ERG waveform predominantly represents outer retina photoreceptor and bipolar cell function, as evidenced from studies on non-human primates under conditions that pharmacologically

isolate the inner and outer retina.[3,4] Additional waveform components such as oscillatory potentials are thought to reflect amacrine and bipolar cells,[5] and the photopic negative response (PhNR) reflects the spiking activity of retinal ganglion cells.[6,7] An alternate way to determine the IRF of a linear system is to measure the response to sinusoidal stimuli at different temporal frequencies and calculate the inverse Fourier transform of this temporal modulation transfer function.[8–11] That these two approaches return different IRFs indicates that the retinal responses are nonlinear, at least with the high-energy stimuli used with the flash ERG.[8–11]

A further method to determine IRFs is to use temporal white noise (TWN) analysis[12] as applied in single cell recordings of spiking activity from retinal ganglion cells.[13] The applicability of white noise analysis in electroretinography has to our knowledge, not been pursued extensively.[14] In the present study, the IRF is obtained by cross-correlating a temporal white noise stimulus (containing all temporal frequencies with equal amplitudes) and the resultant white noise ERG (wnERG) response. Cross-correlation analysis is successfully applied in multifocal ERG (mfERG) recordings[15] to extract responses to flashed stimuli originating in different retinal areas. Since the m-sequence stimulation consists of quasi-random binary stimuli, the resulting mfERG can be considered an array of small flash ERGs.[16] Because the luminance distribution of the TWN stimulus is Gaussian and not binary, the resultant IRF may differ from the flash ERG.

There are fundamental differences between a stimulus flash and temporal white noise that have implications for the resultant ERG response and IRF. First, with flashes, a change in stimulus frequency (when multiple flashes are used) and/or flash strength incurs a change in mean luminance and thus in the level of retinal adaptation. This is not trivial, particularly when the responses are measured after dark adaptation, either necessitating large postflash times for recovery or influencing the measured response if the recovery time is too short. On the other hand, the TWN stimulus can be performed as a modulation around a mean adaptation level, thereby disentangling frequency, contrast, and mean luminance. It cannot, however, be used in the completely dark-adapted retina because the mean adaptation level is a necessary condition. Second, the energy in flash stimuli is strongly compressed in a short time of presentation, and when presented to the dark-adapted eye, it presents an extreme condition, outside the normal operational range in which the retina functions during typical environmental exposures (even if the stimulus is, of course, not hazardous for the healthy retina). The TWN stimulus spreads the energy over time, and the retina gives a response that more closely reflects environmental conditions than the response to one bright flash stimulus. Third, in flash ERGs the response is present within approximately the first 200 ms post stimulus. The remaining time of the interstimulus interval is therefore of no value for the analysis, although the interstimulus interval must be sufficiently long in order to maintain the state of adaptation. In the TWN paradigm, the whole recording period is used in the analysis, thereby increasing the signal-to-noise ratio (SNR) of the recordings. Taken together, the TWN paradigm may present an alternative assay of the integrity of the retina that considers its functional mode of operation during normal environmental light exposure and with a favorable SNR.

The present study provided a preliminary characterization of the electroretinographic IRF in response to a TWN input signal. The first goal was to measure IRFs by independently changing contrast and mean luminance using a TWN analysis. The second goal was to compare the IRFs obtained with TWN and the flash ERG obtained with different spatial and temporal properties. We hypothesized that the TWN and flash IRF would show commonalities in their implicit times and amplitudes of certain waveform components but also that the comparison between the two methods would reveal nonlinear response components in the flash ERG. The third goal was to study the signal distribution of the wnERG; the ERGs elicited by a TWN stimulus were expected to be stochastic, with a distribution that may deviate from Gaussian, which would be informative about the retinal mechanisms involved in the generation of an ERG signal.

Methods

Ethical Approval

The Human Research Ethics Committees at Queensland University of Technology, the University Hospital Erlangen, and the University of Bradford approved all experimental procedures. Participants provided informed consent, and experiments were conducted in accordance with the Code of Ethics of the World Medical Association (Declaration of Helsinki).

Table 1. Recording Conditions in the Different Laboratories

Methods	Brisbane, Australia	Bradford, UK	Erlangen, Germany
ERG type	wnERG	wnERG	Flash ERG
Spatial configuration	39.3°	Full field (Ganzfeld)	40° and full field
Mean luminances, cd.m^{-2}	0.21, 4.12, 41, 130, 260	0.01, 0.1, 1, 10, 16, 32, 48, 64, 100, 200, 300, 400	27, 102, 106.3
Contrasts, % Michelson	40, 36, 32, 28, 24, 20, 16, 12, 8	100, 80, 60, 40, 20	N.A. for flashes
Recording epochs, ms	1000 with 1 ms between epochs	512	1000
Sampling frequency, Hz	1000	1024	2048

N.A., not applicable.

Participants

A total of 13 participants were recruited. The experiments were performed at three different laboratories: (1) At the Institute of Health and Biomedical Innovation, Queensland University of Technology (QUT), Australia; (2) at the School of Optometry and Vision Sciences, University of Bradford, UK; (3) at the Department of Ophthalmology, University Hospital Erlangen, Erlangen, Germany.

All 13 participants underwent a complete ophthalmic examination and had no color vision abnormalities or retinal or systemic disease known to affect the ERG. Of these, five observers were tested using the 39.3° diameter Maxwellian view TWN stimuli in Brisbane (age: 26–39 years; three males, two females); three observers were tested with the full-field (Ganzfeld) TWN stimuli presented in Newtonian view in Bradford (age: 28–48 years; all males); and five participants were tested with a 40° and a full-field flash ERG in Erlangen (age: 28–60 years; one female and four males). The pupil of the tested eye was dilated with tropicamide 0.5% (Bausch & Lomb UK, Ltd., Kingston, UK), and pupil diameter was at least 8 mm for all participants during data collection.

Stimulus Generators

The experiments with white noise stimuli were performed in the laboratories of authors: AJZ and BF in Brisbane (Australia) and DM in Bradford (UK). Flash ERG recordings were performed in the laboratory of JK in Erlangen (Germany). The most important recording conditions in the different labs are summarized in Table 1. In this collaborative project, we employed the optimal conditions and settings to match the recording procedures in each laboratory, which are largely standardized. The main difference was that in Brisbane, 39.3° diameter TWN stimuli were used, and while these closely matched the laboratory conditions in Erlangen (40° diameter), the TWN stimulus was presented in full-field (Ganzfeld) stimulator in Bradford. The flash ERGs recorded in Erlangen were also obtained with full-field stimuli. The stimuli were generated using radiometric and photometrically calibrated multiple primary optical systems. These were specified with reference to the 10° standard Commission Internationale de l'Eclairage (CIE) colorimetric observer (see Ref. 17 for review) to modulate luminance and thus probe ERG responses that accompany activity of the photoreceptor inputs into the inferred magnocellular pathway. The Maxwellian view stimulator in Brisbane was based on a custom-built one-channel optical system.[18] The systems in Bradford and Erlangen used Ganzfeld bowls presented in Newtonian view (in Erlangen: Q450SC; Roland Consult, Brandenburg, Germany; in Bradford: Espion; Diagnosys, Cambridge, UK). All stimuli were produced with narrow-band light-emitting diodes. The spectral outputs of the white adapting lights may differ between the laboratories, but it is expected that this does not have a large effect on the measured responses because all stimuli used isochromatic luminance modulation. The flash ERG paradigm was matched to the mean adaptation level of the white noise paradigm. While these different stimulus setups may introduce differences in amplitudes and implicit times, we would like to emphasize that for comparison between the TWN and flash ERG, the waveforms are described qualitatively and given in arbitrary units. We also evaluated their responses to changing contrast and illuminance.

Electroretinograms

The ERG recording procedures have been described in detail elsewhere.[18–20] Similar recording settings were used in all laboratories. Briefly, continuous ERGs were recorded from one eye in all participants with an active fiber electrode placed

across the lower conjunctiva and attached near the inner and outer canthi according to International Society for Clinical Electrophysiology of Vision (ISCEV) standards.[3] In preparation for the recordings, alcohol and abrasive gel (Nuprep; D.O. Weaver & Co., Aurora, CO) was used to scrub and clean the forehead (ground electrode) and ipsilateral temple (reference electrodes) prior to placement of the silver/silver chloride cup electrodes that were filled with electrode paste (Aquasonic; Parker Laboratories, Inc., Fairfield, NJ). The ERG signals were amplified and filtered between 0.3 and 300 Hz (Brisbane: Grass P511AC amplifier; Grass Technologies AstroMed, Inc., Product Group, Warwick, RI; Erlangen: Roland Consult, and Bradford: Diagnosys) and digitally acquired between 1000 and 2048 Hz.

TWN and the IRF

The TWN stimulus has the property that the amplitude in the frequency domain is equal for all temporal frequencies. The TWN stimuli were therefore generated in the frequency domain by assigning fixed amplitudes to all frequencies between 0 and 512 Hz and a randomly varying phase (0°–360°). It is assumed that higher temporal frequencies are outside the response range of the retina[21] and do not elicit measurable ERG responses. The inverse fast Fourier transform resulted in 1024 luminances at time intervals that were evenly distributed within a 1-second window (in Brisbane, resulting in 0.9766 ms between each renewal of the luminance,[22] and 512 luminances in a 512- ms window in Bradford, that is, a 1-ms interval between time stamps). In the time domain, this resulted in each case in randomly varied luminances that had a Gaussian distribution around the mean luminance. The TWN stimuli were presented in 1-second epochs separated by a 1-ms blank interval and repeated 160 times during each 160-second recording sequence (Brisbane laboratory). The purpose of the 1-ms blank interval is to decorrelate the ERG signal from the line frequency to increase the SNR.[18] Responses to 40 to 160 repetitions of the 512-ms stimulus periods were recorded and averaged (Bradford laboratory). Decorrelation was obtained by using 512-ms epochs. To avoid onset artifacts, the responses to the first two stimulus cycles were discarded.

In both laboratories (Brisbane and Bradford), the ERG to TWN stimuli were measured under steady light-adaptation conditions spanning mesopic and photopic light levels: Brisbane: 0.21 cd.m^{-2} (10 td with an 8-mm diameter pupil), 4.12 (207), 41 (2071), 130 (6550), and 260 cd.m^{-2} (12,570 td); Bradford: 0.01 cd.m^{-2} (0.5 td), 0.1 (5), 1 (50), 10 (503), 16 (804), 32 (1608), 48 (2412), 64 (3216), 100 (5027), 200 (10,053), 300 (15,080), and 400 cd.m^{-2} (20,106 td). Noise contrast was defined as Michelson contrast (C) using the maximal and minimal luminances in the stimulus $\left(C = \frac{(L_{max} - L_{min})}{(L_{max} + L_{min})}\right)$. Observers were light-adapted to the photopic conditions for at least 3 minutes before testing, and between 15 and 30 minutes for the mesopic conditions.

All signal processing was conducted using custom-written Matlab software (R2012a; Mathworks, Natick, MA) and spreadsheets (Excel; Microsoft, Bellvue, WA). After artifact rejection, the data from Brisbane were interpolated to obtain 1024 points per time segment, and the IRF was derived from a cross-correlation between the ERG recording and the TWN stimulus. The data in Bradford were analyzed without preprocessing. In a control experiment, we generated >100 different random phase samples, and there was no difference in the estimated IRF using any of these different TWN stimuli because the power spectral density was constant for all stimuli. Furthermore, we calculated the cross-correlation between a response and a noncorresponding TWN stimulus. This resulted in no or negligibly small IRFs.

Flash Electroretinograms

The flash ERG paradigm (Erlangen laboratory) was matched as closely as possible to the mean adaptation level of the white noise paradigm (Brisbane and Bradford laboratories). Because the standard flash ERG is typically measured to stimuli (≤5-ms duration) of varying strength from a dark or standardized background[3], to generate a set of flash ERG conditions more comparable to the TWN data measured under steady light adaptation, we measured the flash ERG in response to a 5-ms pulse that was periodically repeated every 1000 ms and that was set against a steady adapting field (25 cd.m^{-2} and 100 cd.m^{-2}) (see Fig. 6). The 1000-ms interflash interval was determined to be of sufficient duration to prevent carryover effects of successive flashes on the ERG waveform. Flash strengths were 2 cd.s.m^{-2} for both adapting backgrounds. In addition, a 6.3-cd.s.m^{-2} flash was displayed on the 100-cd.m^{-2} background. Assuming that the retinal adaptation mechanism integrates over a time window that is longer than the 1-second interstimulus interval used in this recording, the adaptation to the flash is similar to a continuous light, with the energy of the flash spread over the whole recording period. Therefore, we

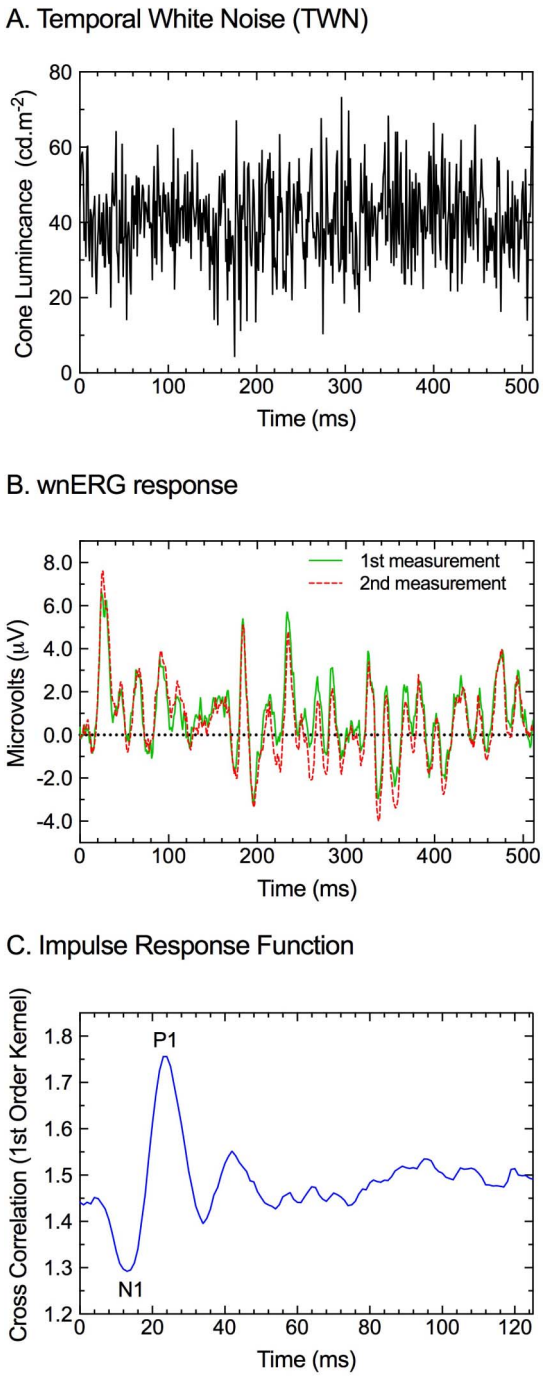

Figure 1. Calculation of the linear IRF (panel C) through the cross-correlation of the temporal white noise stimulus (panel A) and the measured wnERG (panel B). (A) An exemplar TWN stimulus (0–512 Hz) that modulates above and below a mean adaptation level (40 cd.m^{-2}). (B) The measured full-field (Ganzfeld) wnERG responses (two measurements, *green solid* and *red dashed lines*) shown in panel A are the average of 40 sweeps each and are reproducible across repeated measurements. (C) The cross-correlation of the TWN stimulus (panel A) and the resultant wnERG response (panel B) return the linear IRF. Definitions of the N1 and the P1 components are displayed. (Data acquired in the Bradford laboratory).

supposed that the flash gives an additional 2.0 or 6.3 cd.m^{-2} mean luminance, resulting in effective mean luminances of 27, 102, and 106.3 cd.m^{-2}. Assuming a pupil diameter of 8 mm, the effective mean retinal illuminances were approximately 1350, 5130, and 5340 td, respectively. The flash ERG data were the average of at least 20 cycles.

It is important to reemphasize that a comparison between TWN and flash responses are only possible on a qualitative level. TWN stimuli are modulations around a mean adaptation level, whereas the flash stimuli are incremental steps above the adaptation level. The stimulus strength of the former can be expressed in Michelson contrast, whereas the latter should be expressed as a Weber fraction. As a result, with the TWN the mean retinal illuminance is constant for all stimulus contrasts, whereas with flashes the state of adaptation may change with flash strength and frequency. Adaptation is an inherent nonlinearity of the retina and the visual system. Furthermore, the TWN analysis returns the IRF, which is the linear approximation of the ERG response to a Dirac delta function (i.e., infinitely short, infinitely intense, and unit integral of intensity over time). The flash ERG is the measured response to a physical flash and includes many nonlinearities. The comparison of responses to flashes and to TWN stimuli allows for the identification of these non-linearities.

Results

IRFs of the wnERGs

The wnERG response to 40 sweeps of the 512-ms temporal white noise is highly reproducible (Figs. 1A, 1B). To estimate the IRF, the average of the two ERG responses (Fig. 1B) was cross-correlated with the TWN (Fig. 1A) stimulus according to

$$IRF(\tau) = \frac{1}{L}\int_0^L R(t)\cdot S(t-\tau)\cdot dt$$

in which L is the period length, $R(t)$ is the measured response, and $S(t)$ is the TWN stimulus.

The integral was approximated by using the measured potentials at each time interval (1 ms apart):

$$IRF(\tau) = \frac{1}{N}\sum_{n=0}^{N} R(n\cdot\Delta t)\cdot S(n\cdot\Delta t-\tau)$$

where N is the number of time stamps and Δt is the time between two time stamps. The resultant linear

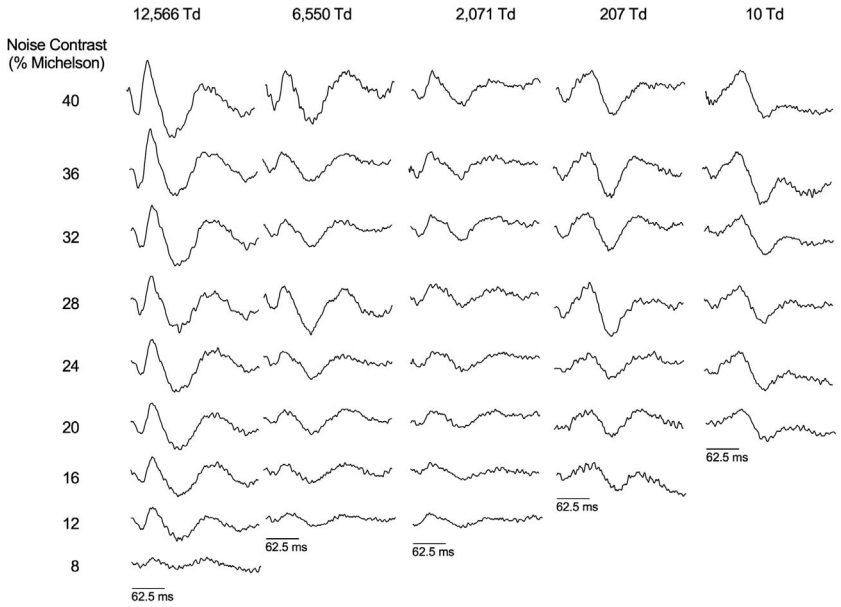

Figure 2. IRFs derived from the TWN ERG with focal (39.3° diameter) stimuli measured in Maxwellian view. Data are for a representative observer. The IRFs are shown for 250-ms duration as a function of Michelson stimulus contrast and adaptation level spanning photopic to mesopic illuminations (Brisbane laboratory).

IRF(τ) (Fig. 1C) calculated in 1-ms steps has an initial negative wave (N1) followed by a positive deflection (P1) and resembles the well-known flash ERG (compare with the flash ERG responses displayed below; see Fig. 6). Furthermore, a second negativity, comparable to the PhNR of the flash ERG, can be observed. However, there are also clear differences with the flash ERG, such as the absence of potentials that are comparable with the oscillatory potentials (OPs). We refrained from using the a- and b-wave descriptors for the wnERG because the physiological origin of these components has not been established. Note that the cross-correlation between stimulus and response is also used in calculating mfERG responses. mfERGs give responses for different spatial locations, whereas the wnERGs presented here do not give spatial information. The second difference is that in most mfERG paradigms the stimulus is binary, with the light either being off or having the maximal intensity, whereas the TWN stimulus is Gaussian distributed around the mean luminance. The local responses in the mfERG recordings therefore resemble the flash ERG.[16,23] We show below that IRFs obtained with the wnERGs may differ from the flash ERG.

The IRFs derived from the cross-correlation between the ERG response and TWN stimulus for one participant for the 39.3° diameter (Fig. 2) and one participant for the full-field (Ganzfeld) stimuli (Fig. 3) show similar IRF waveforms and similar trends in latency and amplitude in response to varying contrast and illuminance. The group data for the 39.3° diameter stimulus are shown Figure 4. The IRFs obtained with the 39.3° stimulus become smaller when the contrasts decrease, thereby validating the method (Fig. 2). At the lowest contrast (8%), the responses are small but clearly measurable. Furthermore, it can be seen that the waveform of the IRF changes in the low mesopic range: At about 10 td, the first a-wave–like (N1) deflection is small, whereas the b-wave–like positivity (P1) is markedly delayed, indicative for intrusion of rod-driven responses. The retinal illuminances at which this component is delayed is comparable to those resulting in delayed b-waves in the flash ERG.[3] The full-field recordings with different contrasts were performed only at a retinal illuminance of 5025 td (100 cd.m^{-2} luminance; Fig. 3). In agreement with the responses to the 39.3° stimuli, a contrast decrease leads to a decrease in response amplitude. Furthermore, the delay in the b-wave–like component at low retinal illuminances can also be observed.

The responses obtained with full fields resemble those with the 39.3° stimuli, except the PhNR-like component is substantially smaller and narrower. Relatively larger PhNRs with spatially restricted stimuli were also found previously when using rapid-on and rapid-off temporal stimulus profiles.[24]

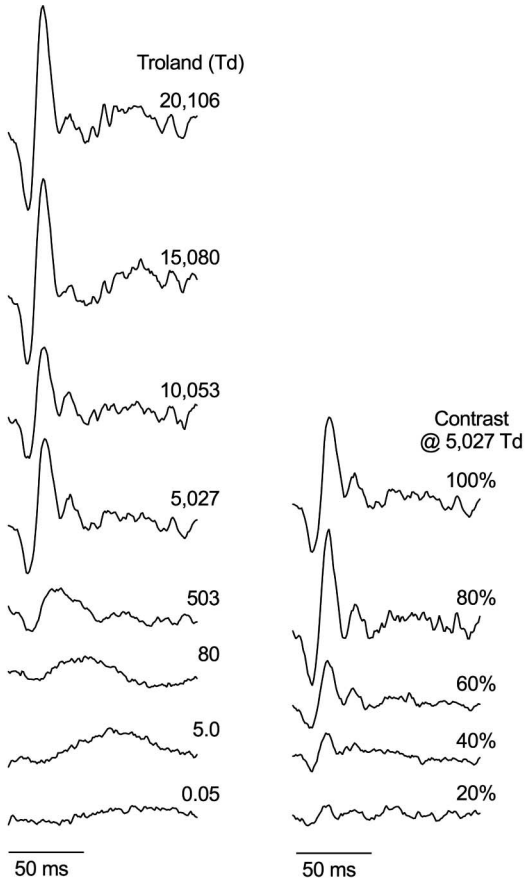

Figure 3. IRFs derived from the TWN ERG with full-field (Ganzfeld) stimuli. Data are for a representative observer. The IRFs are shown for 150-ms duration as a function of the adaptation level (left) spanning photopic to scotopic retinal illuminations (eight light levels: 0.05–20,106 td) for 100% contrast full-field stimuli and as a function of stimulus contrast (with five TWN contrasts at 5027 td; right, Bradford laboratory).

We conclude that the resultant IRFs obtained with TWN stimuli superficially resemble those of the flash ERG and display features that can be expected from a truly physiological response, such as a positive correlation between stimulus contrast and response amplitude and increasing delays of the b-wave homologue at mesopic conditions.

To quantify the relationship between TWN contrast and retinal illuminance (Brisbane laboratory), the average implicit times and amplitudes from five observers are shown in Figure 4 as a function of noise contrast (Figs. 4A, 4B, 4D, 4E) and retinal illuminance at 40% Michelson noise contrast (Figs. 4C, 4F). The N1 (a-wave–like component) implicit times (mean = 15.7 ms ± 1.6 SEM) are relatively constant with varying contrast (Fig. 4A) and adaptation level (Fig. 4E), whereas the P1 (b-wave–like component) implicit time was shorter in photopic illumination (≥2,071 td: mean = 35.7 ± 2.5 ms) than mesopic illumination, for which it became progressively longer with decreasing illumination (207 td: mean = 61.2 ± 3.6 ms; 10 td: mean = 69.4 ± 3.1 ms) independently of noise contrast (Figs. 4B–C). The amplitudes of the two IRF components depend approximately linearly on stimulus contrast; N1 amplitudes show a linear decrease with increasing stimulus contrast (r^2 range, 0.45–0.91), whereas the N1P1 amplitudes show the opposite relationship (r^2 range, 0.70–0.92). At 20% noise contrast, the wnERG was recordable for only one out of five observers (the data for this one observer follow the trends of the average data, but were not included in Fig. 6), and the range of stimulus contrast over which the wnERG was measureable decreased with decreasing illumination.

Figure 5 displays the implicit times (left column) and amplitudes (right column) of the same components of the full-field (Ganzfeld) data (Bradford laboratory) as for the 39.3° focal stimulus (Brisbane laboratory, Fig. 4). In line with the 39.3° data, the implicit times do not change with contrast (μ = 13.8 ms ± 1.1 SEM), whereas the amplitudes depend linearly on stimulus contrast. The lower plots show the data for the 100% contrast responses as a function of mean retinal illuminance (Figs. 5C, 5F). In agreement with the data obtained with the 39.3° stimuli, the implicit times (μ = 24.3 ms ± 0.3 SEM) are constant down to a retinal illuminance of about 500 td, below which they increase substantially (500 td: μ = 33.0 ms ± 2.0 SEM; 5 td: 60.0 ms ± 7.5 SEM). Furthermore, the amplitudes decrease more strongly below 500 td. These data are indicative for a transition between rod and cone–driven responses.

Flash ERGs

Figure 6 shows that typical flash ERG recordings from the Erlangen laboratory measured using both a 40° diameter and full-field (Ganzfeld) stimuli have clear a- and b-waves and are superficially similar to the IRFs obtained with the TWN method (Figs. 2, 3). Importantly, OPs can also be observed, and the PhNRs are similar to those observed in the full-field IRFs (Fig. 3) but are smaller than those seen in the 39.3° IRFs (Fig. 2).

Table 2 summarizes (means ± SD) the amplitudes (μV) and implicit times (ms) of the a-wave (N1) and b-wave (N1P1) components of the flash ERGs obtained from five participants. The responses to the 40° flashes are smaller than responses to the full-field stimuli. Overall, the a-waves were between a factor of

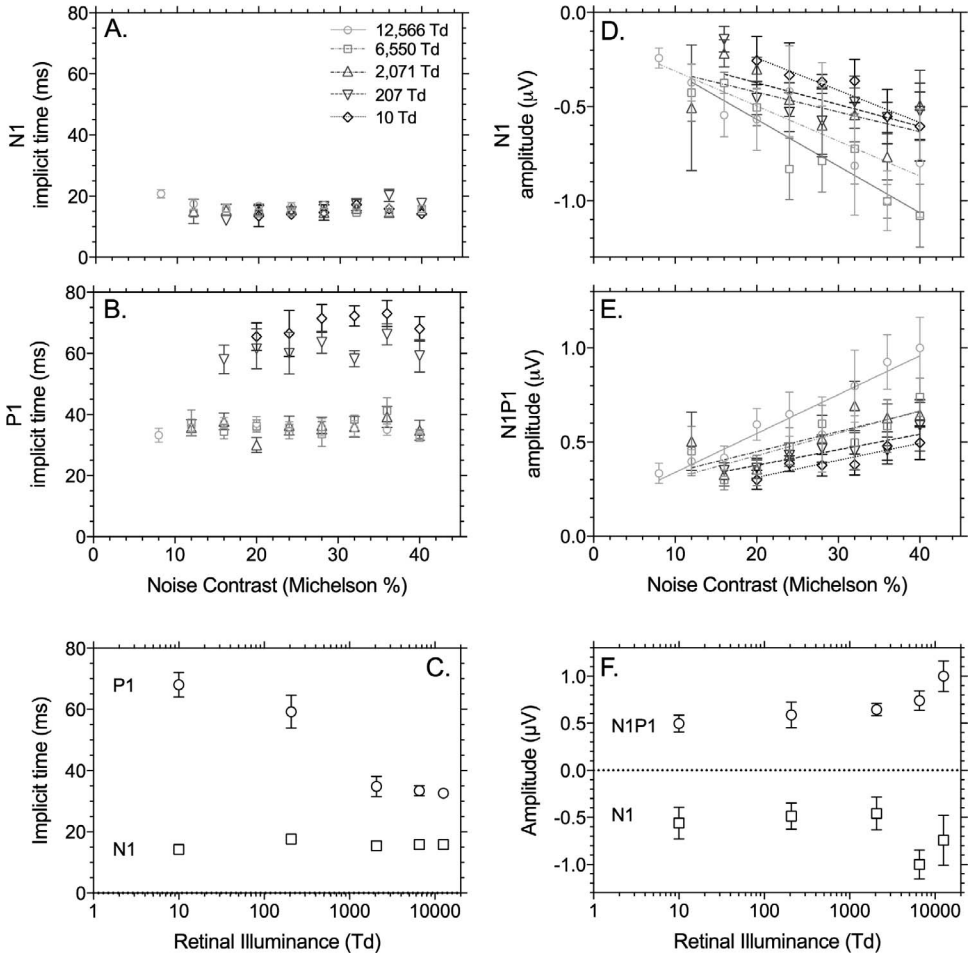

Figure 4. Summary data of the IRF of the wnERG implicit time and amplitude with focal (39.3° diameter) stimuli measured in Maxwellian view (Brisbane laboratory). Data are from the average of five observers (±SEM). Left columns show implicit time (milliseconds) as a function of noise contrast (Michelson %, panels A and B) and retinal illuminance at 40% Michelson noise contrast (panel C). Right columns show the normalized amplitude as a function of noise contrast (Michelson %, panels D and E) and retinal illuminance at 40% Michelson noise contrast (panel F). The amplitudes are normalized to the N1P1 values obtained at 12,566 td and 40% contrast.

2.1 and 3.3 smaller. The b-waves in the 40° responses were between 3.3 and 4.3 times smaller than those in the full-field responses. The implicit times were similar for all flash conditions and corresponded closely to those of their homologues in the IRFs.

Signal Distribution of the wnERG

By definition the TWN stimulus has a Gaussian luminance distribution. The wnERG (Fig. 1B) is also a stochastic signal for which the distribution can be derived using the general principles of signal generation.[12] Therefore, the range of ERG voltages were separated into about 30 bins of equal size, and the number of occurrences within these bins was counted. The distributions of the wnERG from a representative subject (Bradford laboratory) are shown for measurements with 100% contrast stimuli at different luminances and for different contrasts at a 100 cd.m^{-2} mean luminance (Fig. 7). The distribution histograms were fitted with Gaussians, of which the mean (μ) and the standard deviation (σ) were free parameters. Two effects can be observed: (1) The distributions become narrower as luminance or contrast decreases, and thus the responses become smaller; this finding is trivial because the smaller deflections cause a concentration of voltage around the mean. (2) As contrast and particularly luminance decrease, the means of the fitted distributions (i.e., the estimate of the mean voltage) decrease (i.e., the distribution shifts toward lower voltages). This effect is generally present across the three participants in this experiment, as indicated by the positive correlations between the mean voltage on the one hand and mean luminance and contrast on

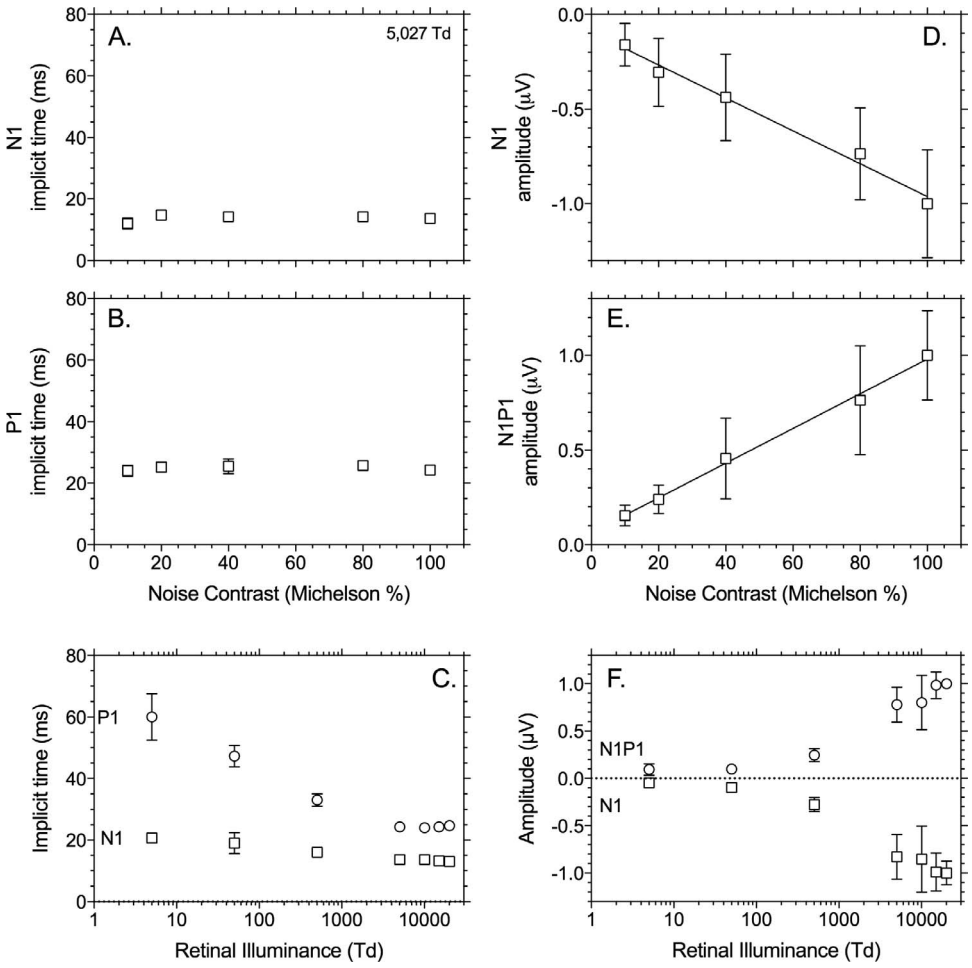

Figure 5. Summary data of the IRF implicit time and amplitude with full-field (Ganzfeld) stimuli. Data are from the average of three observers (±SEM) (Bradford laboratory). Left panels show the implicit time (milliseconds), and right panels show the amplitude normalized to the N1P1 amplitudes obtained at 100% contrast at 20,000 td. Data are plotted as a function of Michelson noise contrast (%) at a single photopic illumination (5025 td) or as a function of retinal illuminance (td) for the highest measured temporal white noise contrast (100%).

the other (Fig. 8). The latter effect indicates that when response amplitudes increase, the increase in electrode positive deflections are larger than the electrode negative deflections.

Discussion

The temporal wnERG paradigm provides an alternate approach to measuring the electrical potential of the eye in response to a flash of light.[1,2] From the cross-correlation between TWN stimuli and the wnERG responses that are elicited by these stimuli, the IRFs are obtained (Fig. 1). The IRFs resemble a waveform similar to the flash ERGs: They contain a- and b-wave–like negative and positive deflections and PhNR-like components.

Differences can be expected between the flash ERG and the IRFs from the wnERG. The latter can be regarded as the linear approximation of the response to a stimulus described by a Dirac delta function (because this function has unity integral, the IRF and the measured response are identical), which in turn is approximated by the flash stimulus in ERG recordings. Therefore, the comparison of IRF from the wnERG with the flash ERG may give additional information on the cellular contributions to the ERG.

The initial corneal negative a-wave of the flash ERG originates from hyperpolarization of rod and cone photoreceptors in response to light and from activity in OFF-bipolar cells[25] (for review see Ref. 26). A-wave amplitudes follow a Naka-Rushton relationship with increasing flash energy,[19] whereas IRF N1 amplitudes increase linearly with TWN

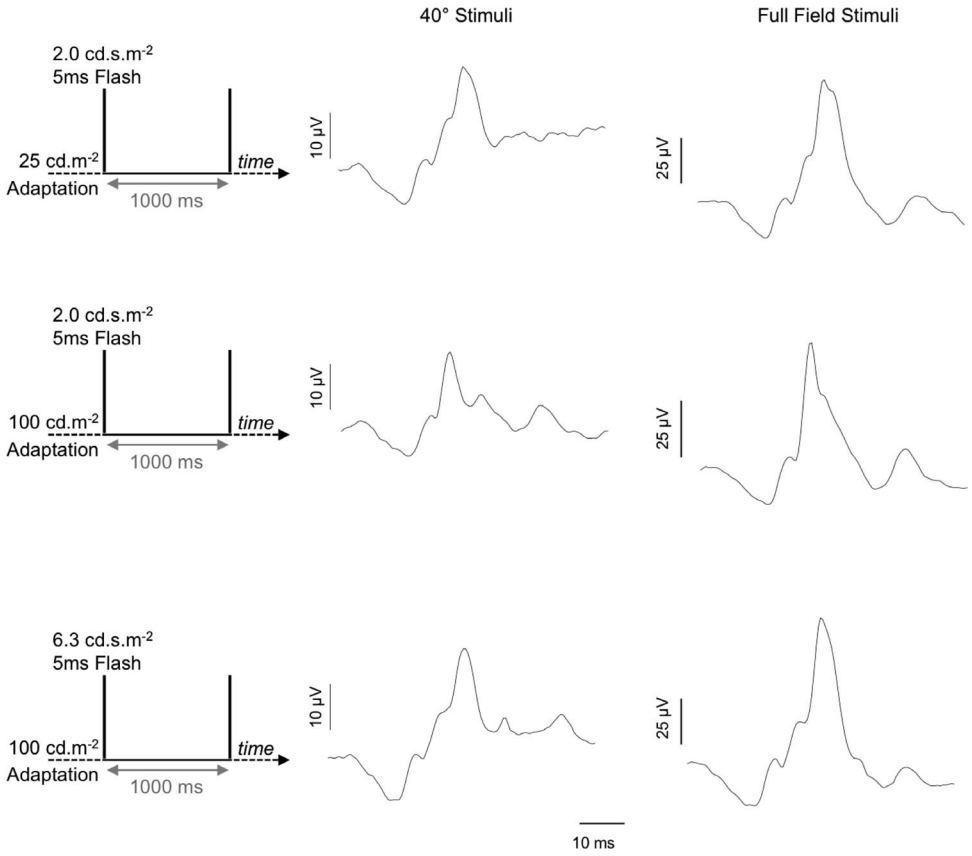

Figure 6. Flash ERG (1-s cycle) waveforms. Stimulus conditions are displayed on the left. Data are for a representative observer (Erlangen laboratory).

contrast over the measured stimulus range (Figs. 4D, 5D), indicating that the response is relatively more linear compared to the flash ERG response. Times to peak of the flash ERG a-wave vary between about 15 and 20 ms, becoming faster with increasing stimulus energy (−1.75 to 3.0 log cd.s.m^2),[19] whereas the wnERG is robust. While rod and cone photoreceptor contributions to the flash ERG must be extracted from flash ERGs recorded to different stimulus wavelengths and irradiances (e.g., photometrically matched long- and short-wavelength flashes under light- and dark-adapted conditions[27,28] or through changes in the timing of successive flashes[29]), the wnERG paradigm can isolate outer retinal photoreceptors by changing the adaptation level; scotopic illumination would be required to measure a rod wnERG. Recently, it was found that rod-driven ERG responses can also be obtained reliably at retinal illuminances up to about 400 td, without the need for extensive dark adaptations.[30,31] It is possible that the

Table 2. Amplitudes and Implicit Times (Means ± SD) of the Flash ERGs (Full Field and 40° Diameter)

		Amplitude and Implicit Time			
Flash ERG Data	Stimulus Size	a-Wave Amplitude, µV	a-Wave IT, ms	b-Wave Amplitude, µV	b-Wave IT, ms
25 cd.m^{-2} adaptation	FF	22.1 ± 10.9	15.1 ± 0.6	98.9 ± 37.4	28.6 ± 1.1
2 cd.s.m^{-2} flash	40°	10.7 ± 7.1	15.4 ± 0.6	26.8 ± 10.4	28.4 ± 1.1
100 cd.m^{-2} adaptation	FF	12.6 ± 4.4	13.7 ± 2.0	66.9 ± 21.7	25.0 ± 1.2
2 cd.s.m^{-2} flash	40°	3.8 ± 4.0	15.7 ± 2.4	15.6 ± 6.8	24.5 ± 1.5
100 cd.m^{-2} adaptation	FF	21.6 ± 9.6	14.5 ± 0.7	105.6 ± 53.3	29.6 ± 1.3
6.3 cd.s.m^{-2} flash	40°	9.2 ± 3.4	15.5 ± 1.9	32.1 ± 17.0	29.7 ± 1.3

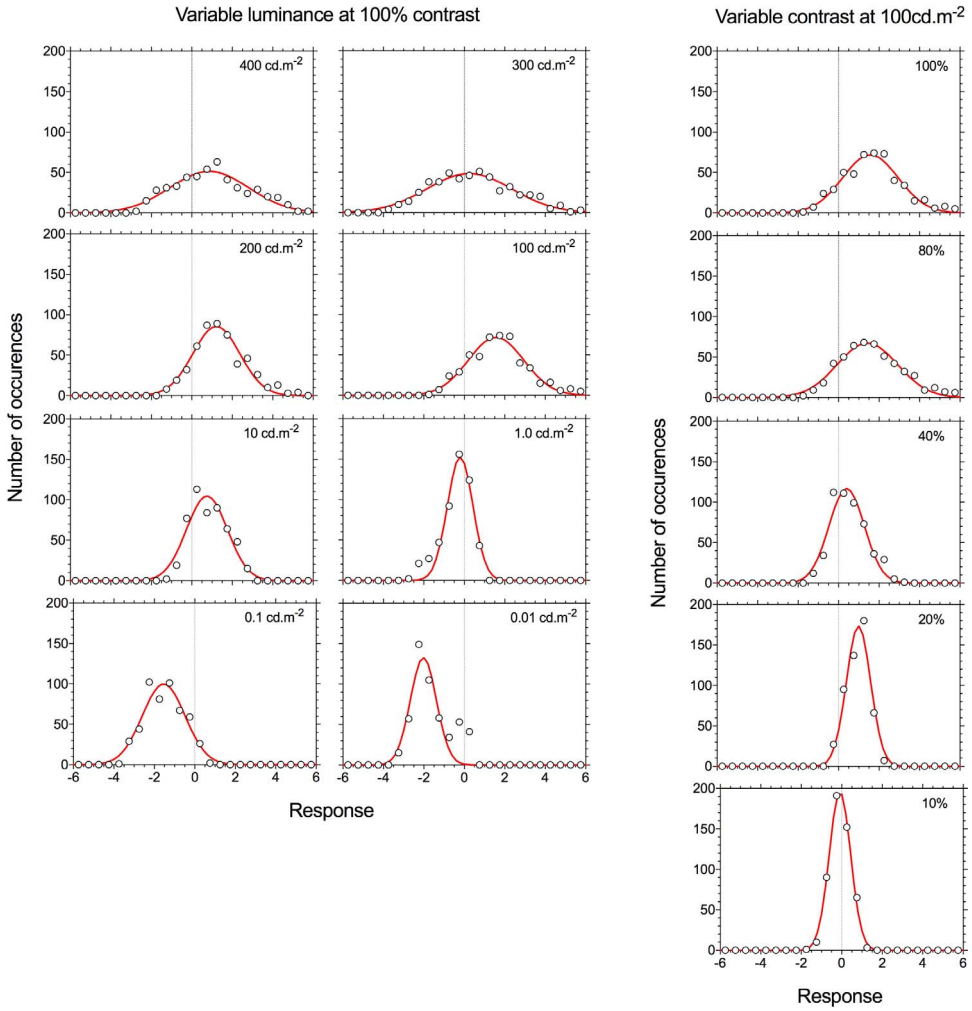

Figure 7. Signal distribution of the wnERG for 100% contrast full-field (Ganzfeld) stimuli (Bradford laboratory) obtained at different mean luminances (400–0.01 cd.m^{-2}) for 100% contrast TWN stimuli (*left*) or with a mean luminance of 100 cd.m^{-2} with TWN stimuli of variable contrasts (10%–100%). The distributions (*circles*) are fitted with Gaussians (*lines*). Data are for a representative observer.

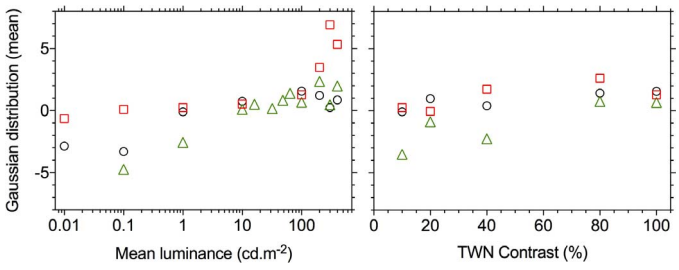

Figure 8. Means (μ) of fitted Gaussians (from Fig. 7) as a function of mean luminance (*left*: fixed 100% contrast) and of TWN contrast (*right*: at a mean luminance of 100 cd.m^{-2}) for three participants (Bradford laboratory). The *circles* show the data for the representative participant from Figure 7. The 100% contrast measurements were also performed at several luminances between 10 and 100 cd.m^{-2} for one participant (*triangular symbols*).

wnERG in combination with the rod-isolating silent substitution is a method to efficiently obtain rod-driven IRFs.

The corneal positive b-wave of the flash ERG is thought to involve ON- and OFF-bipolar cells[32–38] and transretinal currents that depolarize Muller cells.[4,39] Higher stimulus energies produce greater b-wave amplitudes and shorter implicit times,[40] light-adapted photopic b-wave implicit times are approximately 30 to 32 ms, about two times faster than dark-adapted implicit times (approximately 60 ms) but with a 4-fold smaller amplitude. The dark-adapted flash ERG, however, reflects mixed rod and cone responses that depend on flash strength. Here we infer that for all measured adaptation levels, the IRF of the wnERG is dominated by cone signaling, and therefore the shortening P1 implicit time with increasing

illumination (69.4–15.7 ms) may reflect changes in the time constants of post-receptoral processes, such as bipolar cells and rod–cone interactions that delay the time to peak of the cone pathway IRF.[41] While we anticipate that the physiological substrate of the IRFs from the wnERG will show commonalities with the flash ERG and involve photoreceptors and bipolar cells to test hypotheses, primate and rodent models will be necessary, as have been successfully used with flash ERG.[6]

The absence of the OPs on the ascending limb of the N1P1 is a distinct point of differentiation between the IRF from the wnERG and the flash ERG (compare Figs. 2 and 3 with Fig. 6). This is possibly caused by the fact that energy is spread over the whole recording time, whereas with flashes, the energy is concentrated within a short amount of time. Indeed, the OPs manifest in the flash ERG at 100 to 160 Hz[42] and when strong flashes are presented (the threshold for OP responses are stimulus intensities 2.5–3 log units higher than those for b-wave thresholds[5]). OPs are thought to originate in the inner plexiform layer[43,44] and involve negative feedback pathways between bipolar cells, amacrine cells, and ganglion cells. We propose that OPs are an indication of retinal responses to stimulus aspects that are beyond the range encountered in natural scenes and may therefore represent stressed retinal responses. We do not suggest that the OPs do not reflect a physiological mechanism and are meaningless for studying the physiological integrity of the retina. Our inference implies that the OPs were not present in the IRFs of the wnERG because the energy distributions of the temporal white noise stimuli more closely approximate the operating conditions of the retina in natural viewing.

A further aspect that is fundamentally different with wnERGs is the linear relationship between the IRF amplitudes and the stimulus contrast. This is in stark difference to the nonlinear and even non-monotonic relationship between a- and b-wave amplitude and flash strength in the flash ERG. The presence of the so-called photopic hill in the flash ERGs[35,45,46] is another result of the nonlinear behavior of the ERG in response to flashes possibly caused by the compression of stimulus energy. Here we reemphasize that stimulus strength is expressed in different terms in the flash ERG and the wnERG. The TWN stimuli are maximally 100% contrast so that the luminance output can at no time exceed twice the mean output. Flashes can theoretically be infinitely strong. The photopic hill indeed appears with flash strengths of about 0.5 log cd.s.m^{-2},[47] which corresponds to at least 600 cd.m^{-2} (as the ISCEV recommends maximum stimulus durations of 5 ms for the flash ERG). If the background is 30 cd.m^{-2}, as is recommended by the ISCEV for photopic stimulus conditions, then the ratio between stimulus and background is at least 21 ([600 + 30]/30) to be able to observe the photopic hill. This exceeds the maximal ratio of the TWN stimulus by more than a factor of 10.

An important feature of the TWN analysis is that stimulus strength (expressed in terms of contrast) can be varied independently from the mean retinal illuminance and thus the state of adaptation, whereas with flashes they are confounded. The spectral density of the temporal white noise stimulus may also provide a practical alternative for quantifying its strength. Therefore, Figures 4 and 5 display the effects of one variant on the responses. Such graphs cannot be obtained with flash ERGs. The definition of the mesopic range on the basis of the IRF is then fairly straightforward, and the TWN stimulus will allow for parallel exploration of the rod; L-, M-, and S-cone photoreceptor signaling; and postreceptoral magnocellular, parvocellular, and koniocellular pathway processing with multiprimary optical systems,[41,48–50] whereas the single flash ERG on a dark background cannot produce photoreceptor isolation to probe postreceptoral processing. Alternate flash paradigms (e.g., twin flash[29]) are then required to separate rod and cone photoreceptor contributions to the IRF but are measured under different states of light adaptation that frustrates direct comparisons of their temporal characteristics. With such pathway-specific selectivity, there will be obvious benefits of the TWN stimulus for clinical studies evaluating hypotheses related to cellular redundancy to understand the effects of disease on specific pathways. Moreover, the IRF from the wnERG has a high SNR when compared to the measurement recorded in the absence of a stimulus because the wnERG utilizes the entire recording period. Thus, even though the absolute responses to the white noise stimuli are smaller than those in the flash ERGs, the SNR of the IRFs are similar, and responses that were clearly above noise could be obtained with the TWN recordings at contrasts as low as 8%.

Apart from the IRFs, the voltage distributions of the wnERGs are a further analysis method that may offer additional parameters to study the retina. Insights into the component waveforms of the flash ERG have also been provided through time-frequen-

cy analyses with discrete wavelet transforms.[37,38,51] In a purely linear system, the voltage distributions are expected to be Gaussian. Instead, we found that the means of the fitted Gaussians shifted with changing luminance and contrast. These shifts were unexpected because low temporal frequency components, for instance caused by drift, were suppressed by using appropriate filters. It was therefore expected that the means would all be close to 0 μV. The presence of the shift toward positive values at high stimulus contrasts or luminances suggests that positive deflections are favored at high response outputs. These results may point to nonlinearities in the ERG-generating mechanisms, for example, accelerating nonlinearities explaining a facilitation of positive deflections and/or thresholding for the inhibition of negative deflections. However, these nonlinearities are much more subtle than those involved in the generation of the flash ERG.

The wnERG offers new perspectives and additions to the conventional ISCEV flash ERG protocol widely used in human and animal basic and clinical electrophysiology to objectively quantify retinal function. The strongest flash ERG can be inconvenient for a dark-adapted participant and cause blink artifacts. This additionally highlights that flashes are stimulus conditions that are outside the normal modus operandi for the retina. The TWN stimulus minimizes this inconvenience for the observer, thereby limiting the intrusion of these artifacts. Because the entire recording period is used in processing the wnERG, the information for the entire recorded sequence returns a high SNR that can be used to study changes in intrinsic noise in people with retinal disease.[19] In conclusion, the IRFs obtained with the TWN analyses from multiple laboratories using different recording systems, viewing (full-field and focal stimulation), and light-adaptation conditions, validate the technique and demonstrates it is easily translated to new sites for clinical and basic science investigations as a convenient, accurate, and visually relevant manner to study the physiology and pathophysiology of the retina.

Acknowledgments

Supported by Australian Research Council Grant ARC-DP140100333 (AJZ, BF, and JK), IHBI Vision and Eye Program Grant (AJZ and BF), and the German Research Council DFG Grant KR1317/13-1 (JK). We thank Prema Sriram for technical assistance with data collection.

Disclosure: **A.J. Zele**, None; **B. Feigl**, None; **P.K. Kambhampati**, None; **A. Aher**, None; **D. McKeefry**, None; **N. Parry**, None; **J. Maguire**, None; **I. Murray**, None; **J. Kremers**, None

References

1. Granit R. The components of the retinal action potential and their relations to the discharge in the optic nerve. *J Physiol*. 1933;77:207–240.
2. Einthoven W, Jolly WA. The form and magnitude of the electrical response of the eye to stimulation by light at various. *Q J Exp Physiol*. 1908:373–416.
3. McCulloch DL, Marmor MF, Brigell MG, et al. ISCEV Standard for full-field clinical electroretinography (2015 update). *Doc Ophthalmol*. 2015; 130:1–12.
4. Heynen H, van Norren D. Origin of the electroretinogram in the intact macaque eye–I. Principal component analysis. *Vision Res*. 1985; 25:697–707.
5. Wachtmeister L. Oscillatory potentials in the retina: what do they reveal. *Prog Ret Eye Res*. 1998;17:485–521.
6. Frishman LJ. Origins of the electroretinogram. In: Heckenlively JR, Arden GB, eds. *Principles and Practice of Clinical Electrophysiology of Vision*. Cambridge, London: The MIT Press; 2006:139–183.
7. Viswanathan S, Frishman LJ, Robson JG, Harwerth RS, Smith EL. The photopic negative response of the macaque electroretinogram: reduction by experimental glaucoma. *Invest Ophthalmol Vis Sci*. 1999;40:1124–1136.
8. Watson AB. Temporal sensitivity. In: Boff KR, Kaufman L, Thomas JP, eds. *Sensory Processes and Perception*. New York: Wiley-Verlag; 1986:1–43.
9. Kremers J, Lee BB, Pokorny J, Smith VC. The responses of macaque retinal ganglion cells to complex temporal waveforms. In: Valberg A, Lee BB, eds. *From Pigments to Perception. Advances in Understanding Visual Processes*. New York: Plenum Press; 1991:1–9.
10. Kremers J, Lee BB, Pokorny J, Smith VC. Responses of macaque ganglion cells and human

observers to compound periodic waveforms. *Vision Res*. 1993;33:1997–2011.
11. Lee BB, Pokorny J, Smith VC, Kremers J. Responses to pulses and sinusoids in macaque ganglion cells. *Vision Res*. 1994;34:3081–3095.
12. Marmarelis PZ, Marmarelis VZ. *Analysis of Physiological Sys*tems. New York: Plenum Press; 1978.
13. Field GD, Gauthier JL, Sher A, et al. Functional connectivity in the retina at the resolution of photoreceptors. *Nature*. 2010;467:673–677.
14. Saul AB, Still AE. Multifocal electroretinography in the presence of temporal and spatial correlations and eye movements. *Vision*. 2017;1:3.
15. Sutter EE, Tran D. The field topography of ERG components in man–I. The photopic luminance response. *Vision Res*. 1992;32:433–446.
16. Hood DC. Assessing retinal function with the mulifocal technique. *Prog Retin Eye Res*. 2000;19: 607–646.
17. Zele AJ, Cao D. Vision under mesopic and scotopic illumination. *Front Psychol*. 2015;5:1594.
18. Zele AJ, Feigl B, Kambhampati PK, Hathibelagal AR, Kremers J. A method for estimating intrinsic noise in electroretinographic (ERG) signals. *Doc Ophthalmol*. 2015;131:85–94.
19. Kremers J, Jertila M, Link B, Pangeni G, Horn FK. Spectral characteristics of the PhNR in the full-field flash electroretinogram of normals and glaucoma patients. *Doc Ophthalmol*. 2012;124:79–90.
20. Kremers J, Link B. Electroretinographic responses that may reflect activity of parvo- and magnocellular post-receptoral visual pathways. *J Vis*. 2008;8:1–14.
21. Smith VC, Pokorny J, Lee BB, Dacey DM. Sequential processing in vision: the interaction of sensitivity regulation and temporal dynamics. *Vision Res*. 2008;48:2649–2656.
22. Hathibelagal AR, Feigl B, Kremers J, Zele AJ. Correlated and uncorrelated invisible temporal white noise alters mesopic rod signaling. *J Opt Soc Am A*. 2016;33:A93–103.
23. Hood DC, Seiple W, Holopigian K, Greenstein VC. A comparison of the components of the multifocal and full-field ERGs. *Visual Neurosci*. 1997;14:533–544.
24. Tsai TI, Jacob MM, McKeefry D, Murray IJ, Parry NRA, Kremers J. Spatial properties of L- and M-cone driven incremental (On-) and detrimental (Off-) electroretinograms: evidence for the involvement of multiple post-receptoral mechanisms. *J Opt Soc Am A*. 2016;3:A1–A11.
25. Murakami M, Kaneko A. Subcomponents of P3 in cold-blooded vertebrate retinae. *Nature*. 1966; 2:103–104.
26. Lamb TD, Pugh EN. Dark adaptation and the retinoid cycle of vision. *Prog Retin Eye Res*. 2004; 23:307–380.
27. Hood DC, Birch DG. Human cone receptor activity: the leading edge of the a-wave and models of receptor activity. *Visual Neurosci*. 1993; 10:857–871.
28. Hood DC, Birch DG. Light adaptation of human rod receptors: the leading edge of the human a-wave and models of rod receptor activity. *Vision Res*. 1993;33:1605–1618.
29. Pepperberg DR, Birch DG, Hood DC. Photoresponses of human rods in vivo derived from paired-flash electroretinograms. *Visual Neurosci*. 1997;14:73–82.
30. Maguire J, Parry NR, Kremers J, Kommanapalli D, Murray IJ, McKeefry DJ. Rod electroretinograms elicited by silent substitution stimuli from the light-adapted human eye. *Trans Vis Sci Technol*. 2016;5(4):13.
31. Maguire J, Parry NR, Kremers J, Murray IJ, McKeefry D. The morphology of human rod ERGs obtained by silent substitution stimulation. *Doc Ophthalmol*. 2017;134:11–24.
32. Sieving PA, Murayama K, Naarendorp F. Push-pull model of the primate photopic electroretinogram: a role for hyperpolarizing neurons in shaping the b-wave. *Visual Neurosci*. 1994;11: 519–532.
33. Furukawa T, Hanawa I. Effects of some common cations on electroretinogram of the toad. *Jpn J Physiol*. 1955;5:289–300.
34. Pepperberg DR, Masland RH. Retinal-induced sensitization of light-adapted rabbit photoreceptors. *Brain Res*. 1978;151:194–200.
35. Kondo M, Piao CH, Tanikawa A, Horiguchi M, Terasaki H, Miyake Y. Amplitude decrease of photopic ERG b-wave at higher stimulus intensities in humans. *Jpn J Ophthalmol*. 2000;44:20–28.
36. Ueno S, Kondo M, Niwa Y, Terasaki H, Myake Y. Luminance dependence of neural components that underlies the primate photopic electroretinogram. *Invest Ophthalmol Vis Sci*. 2004;45:1033–1040.
37. Gauvin M, Little JM, Lina JM, Lachapelle P. Functional decomposition of the human ERG based on the discrete wavelet transform. *J Vis*. 2015;15:14.
38. Gauvin M, Sustar M, Little JM, Brecelj J, Lina JM, Lachapelle P. Quantifying the ON and OFF

contributions to the flash ERG with the discrete wavelet transform. *Trans Vis Sci Technol*. 2017; 6(1):3.
39. Miller RF, Dowling JE. Intracellular responses of the Müller (glial) cells of mudpuppy retina: their relation to b-wave of the electroretinogram. *J Neurophysiol*. 1970;33:323–341.
40. Dodt E. Beitraege zur Elektrophysiologie des Auges. I. Mitteilung: Ueber die sekundaere Erhebung im Aktionspotential des menschlichen Auges bei Belichtung. *Graefe's Arch Klin Exp Ophthalmol* 1951;151:672–692.
41. Zele AJ, Cao D, Pokorny J. Rod-cone interactions and the temporal impulse response of the cone pathway. *Vision Res*. 2008;48:2593–2598.
42. Asi H, Perlman I. Relationships between the electroretinogram a-wave, b-wave and oscillatory potentials and their application to clinical diagnosis. *Doc Ophthalmol*. 1992;79:125–139.
43. Wachtmeister L, Dowling JE. The oscillatory potentials of the mudpuppy retina. *Invest Ophthalmol Vis Sci*. 1978;17:1176–1188.
44. Ogden TE. The oscillatory waves of the primate electroretinogram. *Vision Res*. 1973;13:1059–1074.
45. Wali N, Leguire LE. The photopic hill: a new phenomenon of the light adapted electroretinogram. *Doc Ophthalmol*. 1992;80:335–345.
46. Rufiange M, Rousseau S, Dembinska O, Lachapelle P. Cone-dominated ERG luminance-response function: the Photopic Hill revisited. *Doc Ophthalmol*. 2002;104:231–248.
47. Rufiange M, Dumont M, Lachapelle P. Modulation of the human photopic ERG luminance-response function with the use of chromatic stimuli. *Vision Res*. 2005;45:2321–2330.
48. Zele AJ, Maynard ML, Feigl B. Rod and cone pathway signaling and interaction under mesopic illumination. *J Vis*. 2013;13:21.
49. Huchzermeyer C, Kremers J. Perifoveal S-cone and rod-driven temporal contrast sensitivities at different retinal illuminances. *J Opt Soc Am A Opt*. 2017;34:171–183.
50. Cao D, Pokorny J, Grassi MA. Isolated mesopic rod and cone electroretinograms realized with a four-primary method. *Doc Ophthalmol*. 2011;123: 29–41.
51. Varadharajan S, Fitzgerald K, Lakshminarayanan V. A novel method for separating the components of the clinical electroretinogram. *J Mod Opt*. 2007;54:1263–1280.